Journal of Materials Chemistry C

Accepted Manuscript

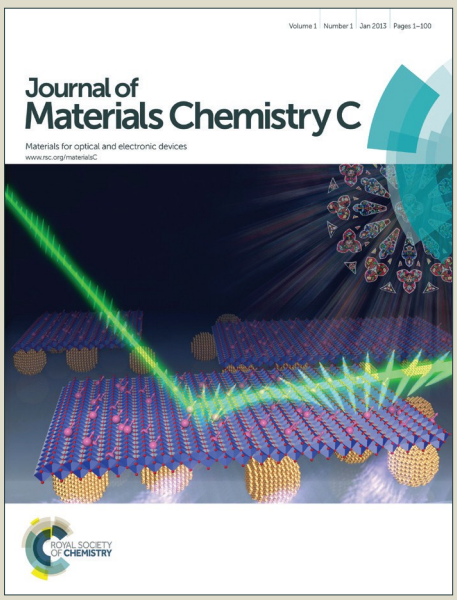

This is an *Accepted Manuscript*, which has been through the Royal Society of Chemistry peer review process and has been accepted for publication.

Accepted Manuscripts are published online shortly after acceptance, before technical editing, formatting and proof reading. Using this free service, authors can make their results available to the community, in citable form, before we publish the edited article. We will replace this *Accepted Manuscript* with the edited and formatted *Advance Article* as soon as it is available.

You can find more information about *Accepted Manuscripts* in the Information for Authors.

Please note that technical editing may introduce minor changes to the text and/or graphics, which may alter content. The journal's standard Terms & Conditions and the Ethical guidelines still apply. In no event shall the Royal Society of Chemistry be held responsible for any errors or omissions in this *Accepted Manuscript* or any consequences arising from the use of any information it contains.

ROYAL SOCIETY OF CHEMISTRY

www.rsc.org/materialsC

Journal Name

ARTICLE

Rational Design of Diketopyrrolopyrrole-based Oligomers with Deep HOMO Level and Tunable Liquid Crystal Behavior by Modulating the Sequence and Strength of Donor Moiety

Received 00th January 20xx,
Accepted 00th January 20xx

DOI: 10.1039/x0xx00000x

www.rsc.org/

Jin-Liang Wang,* Zheng-Feng Chang, Xiao-Xin Song, Kai-Kai Liu, Ling-Min Jing

A family of narrow-band gap π-conjugated oligomers and isomers based on diketopyrrolopyrrole and difluorobenzothiadiazole coupled with oligothiophene or thiazole ring have been successfully synthesized. They exhibited intensive absorption bands (300～900 nm) and deep-lying HOMO energy levels (-5.41～-5.60 eV) due to donor-acceptor interaction and multiple fluorine substituents. The sequence and intensity of electron donor moiety play an important role in determining bulk molecular properties, such as the photophysical properties, the HOMO/LUMO energy levels and mesomorphic properties. Compared with isomer **DTFB2T**, **D2TFBT** with two *n*-hexyl-substituted thiophene as the terminal groups exhibited good liquid crystal behavior with Smectic phase when cooled from 180 °C, and it generated a large area of the liquid-crystalline phase at about 100 °C. However, we did not observe such behaviors in **DTFB2T** due to the different sequence of moiety.

Introduction

Solution-processed organic solar cells (OSCs) with π-conjugated polymer or oligomers as donor have attracted considerable attention as an effective technology for using sunlight because of their advantages such as light weight, flexibility, and low cost.[1-8] Recently, solution-processed narrow-band gap oligomers have gained increasing research interest because of their unique advantages, such as simple purification, monodisperse structures, no end-group contaminants, and reduced batch-to-batch variability compared to polymer materials.[9-20] The functional oligomers have been widely used in organic electronic devices, such as organic photovoltaics (OPV) and organic field-effect transistors(OFET).[21-34] Meanwhile, the thermal-reversible π-conjugated polymer or oligomers in liquid-crystal (LC) for high degrees of order and extensive π-orbital overlap lead to high intrachain charge-carrier mobilities.[35]

Diketopyrrolopyrrole (DPP), with two fused electron-deficient lactams, is a typical strong acceptor chromophore with high molar extinction coefficient. Thus it has been widely investigated in oligomers organic solar cells with high short circuit current density.[36-41] However, open circuit voltage of devices from these compounds is usually low due to elevation of the HOMO energy level of the donor with DPP units, which is the great challenge for DPP-based oligomers to further improve performance of device. Indeed, it is well known that the HOMO levels and the LUMO levels are important for organic photovoltaics materials. Consequently, a careful choice of donor and acceptor subunits and their sequence in synthesis of π-conjugated oligomers with intriguing molecular properties such as deep energy level is highly desirable and worthy of in-depth investigation.

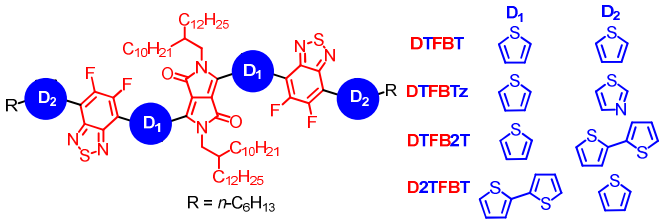

Chart 1. Structures of π-conjugated oligomers **DTFBT**, **DTFBTz**, **DTFB2T** and **D2TFBT**.

Herein, we describe the design, and synthesis a series of π-conjugated oligomers based on D_2-A_2-D_1-A_1-D_1-A_2-D_2 molecular skeletons, as shown in Chart 1. All of the target molecules have a DPP-based core as the central stronger acceptor unit (A_1), two oligomeric thiophene as the donor (D_1), with two difluorobenzothiadiazole as the weaker acceptor (A_2), and two oligomeric thiophene or thiazole as the terminal groups (D_2).

Beijing Key Laboratory of Photoelectronic/Electrophotonic Conversion Materials, Key Laboratory of Cluster Science of Ministry of Education, School of Chemistry, Beijing Institute of Technology, Beijing, 100081, China
E-mail: jinlwang@bit.edu.cn

Journal of Materials Chemistry C Accepted Manuscript

We focus our studies on evaluating how structural variations affect molecular properties in two aspects: (1) variation of ability of terminal electron-donor groups through replacing the two thiophenes by two thiazoles to control the molecular energy levels, optical properties; (2) variation of the length

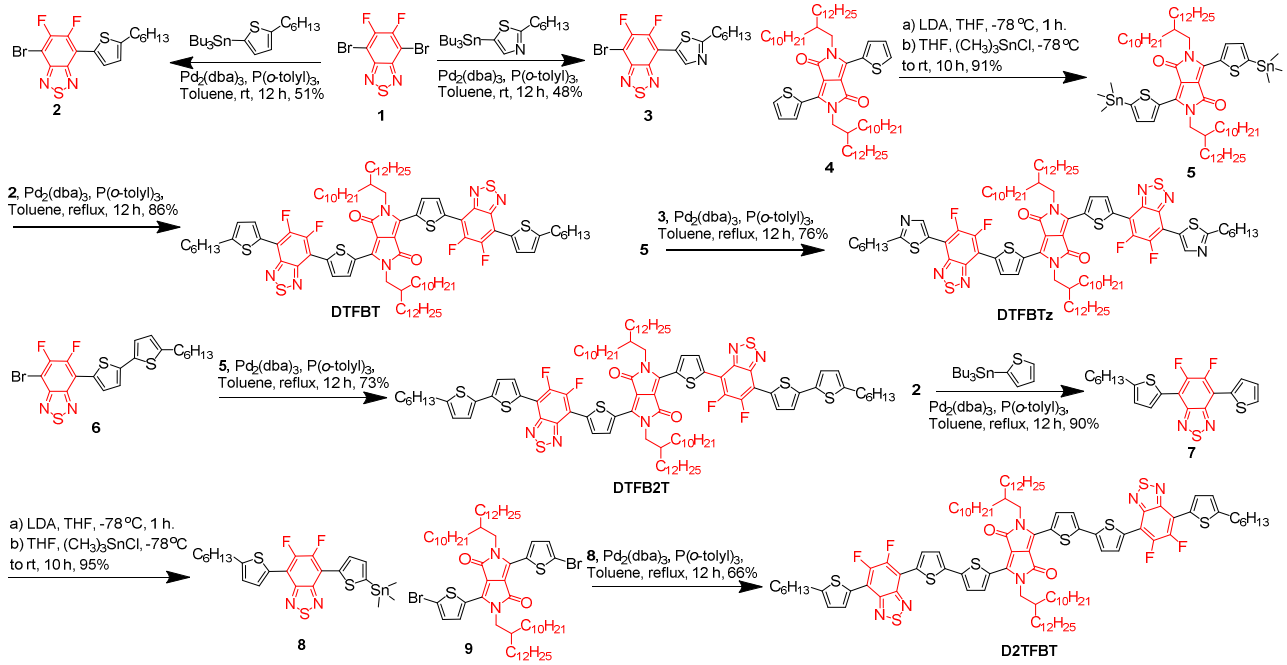

Figure 1. Synthesis of these π-conjugated oligomers **DTFBT**, **DTFBTz**, **DTFB2T** and **D2TFBT**.

of π-bridge unit between two acceptor chromophores by exchanging difluorobenzothiadiazole and thiophene positions to change the light-harvesting ability, phase-transition properties, and the HOMO/LUMO energy level. Such tunable absorption bands and energy levels might bring insight into the synthesis of diketopyrrolopyrrole-based oligomers for organic electronic devices.

Results and Discussion

The synthetic routes to these DPP-based oligomers are shown in Figure 1. The monobromide intermediate **2** was prepared through the Stille coupling reactions by tributyl(5-hexylthiophen-2-yl)stannane[42] and 4,7-dibromo-5,6-difluorobenzo[c][1,2,5]thiadiazole (**1**)[43] in 51% isolated yield. Similarly, **3** was afforded by 2-hexyl-5-(tributylstannyl)thiazole[44] and **1** in 48% isolated yield. Then **4**[45] can be lithiated by LDA followed by quenching with trimethyltin chloride to afford ditin reagent **5** that was directly used in the next step without any further purification. **DTFBT** was obtained through two-fold Stille coupling reaction between the ditin reagent **5** and monobromide **2** as dark solid in 86% isolated yield. Similarly, **DTFBTz** was synthesized between **5** and **3** as dark solid in 76% isolated yield. Moreover, **DTFB2T** with two *n*-hexyl-substituted bithiophene as the terminal groups was obtained between 5 and **6**[46] as dark solid in 73% isolated yield. **7** was prepared by a Stille coupling reaction between **2** and 2-tributyltinthiophene in 90% isolated yield. Treatment of **7** with LDA followed by trimethyltin chloride and recrystallized from methanol and chloroform to afford the target product **8** as red solid in 95% isolated yield. Finally, **D2TFBT** with two *n*-hexyl-substituted thiophene as the terminal groups was obtained between **8** and **9**[45] as dark solid in 66% isolated yield. All compounds were purified by silica gel column chromatography, and their structures and purity were verified by ^{1}H and ^{13}C NMR, elemental analysis, and ESI/MALDI-TOF MS.

The absorption spectra of these π-conjugated oligomers both in diluted chloroform solutions and in thin films obtained by spin-coating were recorded in Figure 2. All oligomers showed two distinct absorption bands (Band I: 300-550 nm; Band II: 550-900 nm) in solution and solid state due to π-π* transition of conjugated backbone for Band I and the intramolecular charge transfer (ICT) between molecular donor and acceptor unit Band II. In solution, very interestingly, although the λ_{max} of **DTFBTz** in Band II region is nearly identical to that of **DTFBT**, introduction of nitrogen atoms in **DTFBTz** exhibited a noticeable blue-shift by ca. 8 nm at λ_{max} in Band I region and obvious increases of the molar extinction coefficient values both Band I and II in comparison with **DTFBT**. Moreover, **DTFB2T** with bithiophene ring as the terminal donor group display the λ_{max} at 475 nm and 650 nm along with an obvious increase of absorbance intensity, which showed red-shift of 26 nm, and 18 nm in comparison with **DTFBT** due to increase of the effective conjugation length, respectively. As compared with **DTFB2T**, the maximum absorption peaks (λ_{max}) of **D2TFBT** were located at about 466 nm and 630 nm and caused dramatically blue shift by ca. 9 and 20 nm, respectively. Obviously, such spectra differences in solution

This journal is © The Royal Society of Chemistry 20xx

Journal of Materials Chemistry C Accepted Manuscript

are because of the structure variations between **D2TFBT** and **DTFB2T**, in which difluorobenzothiadiazole and one thiophene unit exchanged their positions. It is probably that **D2TFBT** have weaker interaction between the DPP and difluorobenzothiadiazole by longer thiophene spacer, which also reduced intensity of intramolecular charge transfer (ICT) between the donor and acceptor groups. Moreover, compared with **D2TFBT** and **DTFB2T** with bithiophene spacer, somewhat better resolved vibronic structure near the wavelength of maximum absorption are shown in **DTFBTz** and **DTFBT**, which might be attributed to the increase of molecular rigidity and planarity through the fluorine-sulfur or fluorine-hydrogen interactions between benzothiadiazole and single thiophene ring.[47-49]

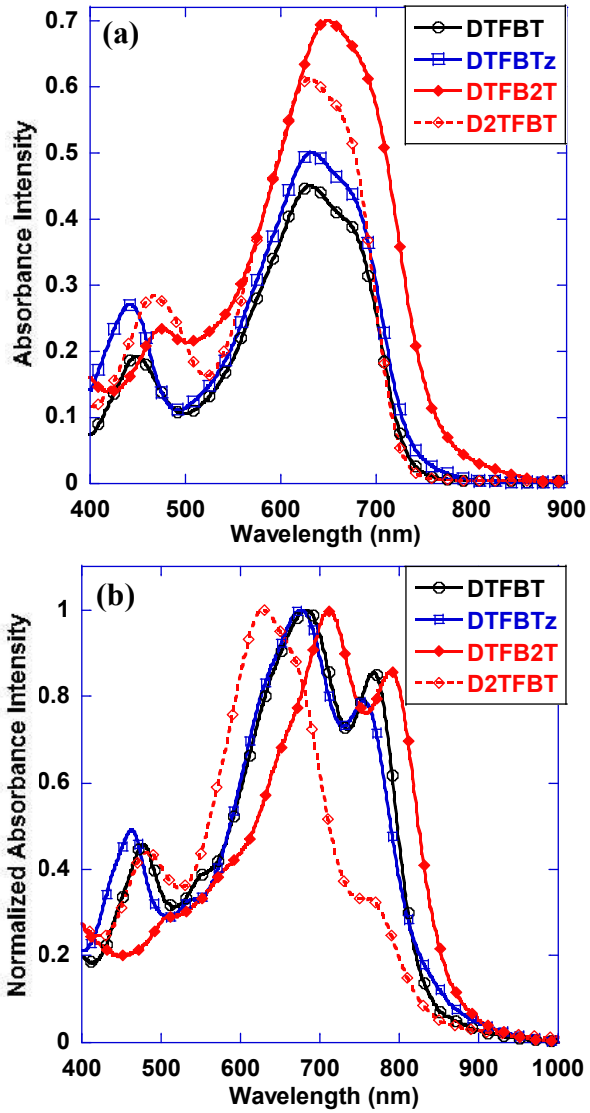

Figure 2. The absorption spectra of π-conjugated oligomers (a) in chloroform solutions (2×10^{-6} M) and (b) in the thin films.

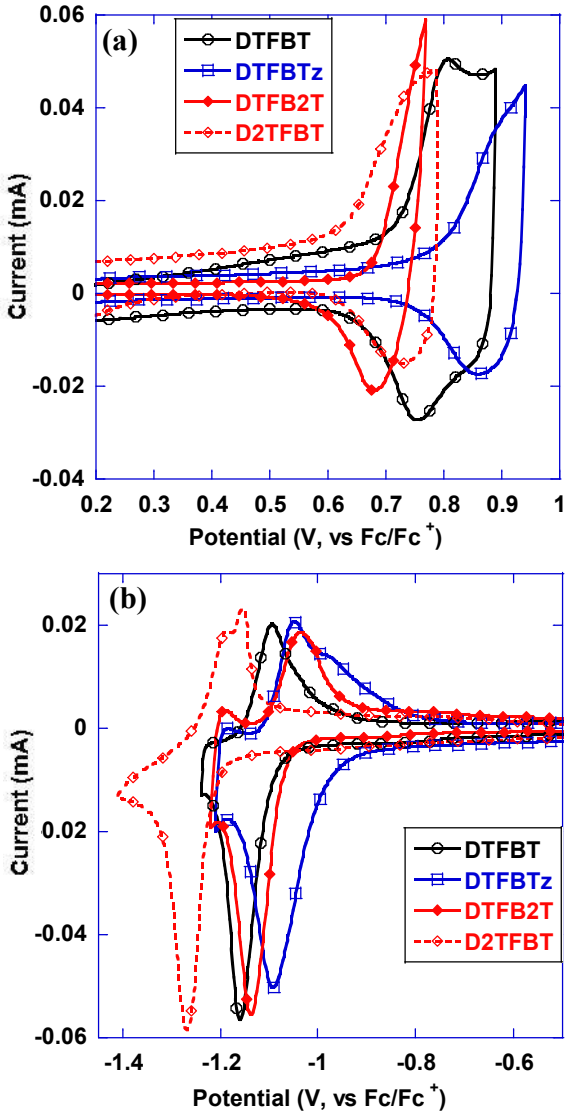

Figure 3. Cyclic voltammogram of π-conjugated oligomers films on Pt electrode in 0.1 M Bu_4NPF_6 in CH_3CN solution.

In contrast, the absorption spectra of these π-conjugated oligomers in thin films are obvious red-shifted with shoulder features in comparison with those of in diluted solution. For example, compared with those absorption maximum in solutions, **DTFBTz** and **DTFBT** showed red-shift of ca. 46 nm and 48 nm, respectively, whereas the thin film of **DTFB2T** displays the largest red-shift of 62 nm on the maximum absorption peak (λ_{max}) and exhibits most obvious 0-0 vibrational peak (shoulder peaks) relative to those of solutions among these three materials. Such features are attributed to a more planar conjugated backbone and *J*-aggregation (slipped) in the solid state.[50] Therefore, a higher π-electron delocalization through the whole molecular backbone and enhanced interchromophore interactions is expected, which could be beneficial to light-harvesting process. However, compared to the diluted solution, it is noted that **D2TFBT**

Journal of Materials Chemistry C Accepted Manuscript

exhibited a slight blue-shift of λ_{max} peak in Band II region with a concomitant less intense peak at longer wavelengths in the solid state. These changes implied that the intermolecular aggregation of **D2TFBT** might be suppressed in films.[51] Moreover, compared with **DTFB2T,** λ_{max} peak of **D2TFBT** showed dramatically blue-shift of ca. 86 nm in solid state, which indicated that **D2TFBT** has weaker intermolecular interactions than **DTFB2T** due to the formation of different types of staking**.** From the onset of absorption, the optical band gap of thin films were estimated to be 1.52 eV for **DTFBT**, 1.51 eV for **DTFBTz**, 1.46 eV for **DTFB2T,** and 1.48 eV for **D2TFBT**, respectively. Moreover, these oligomers were nonluminescent in thin films due to efficient interchain interaction and feature of intramolecular charge transfer in the solid state. It is clear that **DTFB2T** has the relative broad absorption among these materials in thin films and that is preferable to donor materials of organic solar cells.

In order to get insight into the relationship between the chemical structures and the electrochemical properties of the desired materials, the cyclic voltammetry (CV) experiments of these materials in thin films were conducted. The CV curves of these oligomers showed one quasi-reversible *p*-doping process and *n*-doping process (Figure 3). The HOMO and LUMO levels are -5.53 eV/-3.71 eV for **DTFBT**, -5.60 eV/-3.80 eV for **DTFBTz**, -5.48 eV/-3.72 eV for **DTFB2T**, and -5.43 eV/-3.59 eV for **D2TFBT**, respectively, according to the following equation of E_{HOMO} = -e(E_{ox}+4.80) (eV) and E_{LUMO} = -e(E_{red}+4.80) (eV). **DTFBTz** showed markedly deeper HOMO and LUMO energy levels (ΔE = 0.07 and 0.09 eV) relative to that of **DTFBT** as a consequence of replacing thiophene ring by thiazole ring on the terminal units to enhance the electron-deficient property.[52] Introduction of the extra thiophene units on the terminal units caused slightly increase in the HOMO energy levels of **DFB2T** with respect to the **DTFBT** due to enhancing the donor ability by thiophene units. In the contrast, **D2TFBT** with bithiophene spacer between DPP and difluorobenzothiadiazole exhibited obviously higher HOMO/LUMO energy levels, particular for LUMO, compared with that of isomer of **DTFB2T** due to enhancing the donor ability by thiophene units, which is also supported by theoretical calculations as discussed below. The electrochemical band gaps ($E_{g(cv)}$) albeit slightly larger than the corresponding optical band gaps ($E_{g(opt)}$) because of somewhat different measured states.

To further understand the influence of exchanging difluorobenzothiadiazole and one thiophene unit on both the backbone conformation and molecular properties of two isomers **DTFB2T** and **D2TFBT**, the geometries and the respective frontier orbital distributions of two isomers were optimized with DFT B3LYP/6-31G(d) method. In the DFT calculations the side-chains on the DPP and terminal groups were replaced by menthyl group to improve computational efficiency. Although two materials exhibited a good planar structure for π-conjugation, there are subtle different in dihedral angles among the moieties. For **D2TFBT**, four dihedral angles from cientral DPP to the end of thienyl unit are 5, 6, 0, 2°, respectively, whereas these angles are 7, 3, 2, 10° for **DTFB2T** (see Figure S1). Such difference may affect molecular packing structure in the solid state, and then influence their molecular properties. The HOMO and LUMO of **DTFB2T** is almost delocalized along the entire backbone except to the terminal thienyl unit(see Figure 4), In contrast for **D2TFBT**, a much stronger localization of HOMO around the central bithiophene functionalized DPP core and much better delocalization of LUMO are observed. Such difference may cause the obviously higher calculated LUMO/HOMO energy levels of **D2TFBT,** which is consistent with the CV results.

The thermal property of these oligomers was investigated by thermogravimetric analysis (TGA) (Figure 5). Under N_2 atmosphere, the onset temperature with 5% weight-loss was at about 404 °C for **DTFBT**, 382 °C for **DTFBTz,** 411 °C for **DTFB2T,** 408 °C for **D2TFBT,** respectively, which indicated that the thermal stability of these molecules is adequate for application in organic solar cells. We further investigated phase-transition properties of isomers **DTFB2T** and **D2TFBT** by differential scanning calorimetry (DSC) (Figure 6). **D2TFBT** displayed a sharp endothermic peak at ca. 198 °C and a sharp exothermic peak at 191 °C in the second heating-cooling cycle, which is attributed to melting and crystallizing phase transition. Moreover, a pair of weaker thermal transition at around 130 °C was also observed for **D2TFBT,** which might originate from mesophase transitions. In comparison, **DTFB2T** only exhibited a higher temperature of melting/crystallizing phase transition at about 207 °C/202 °C. These results indicated that the isomer **DTFB2T** has stronger intermolecular interaction than **D2TFBT.**

Table 1. Photophysical and electrochemical properties of these π-conjugated oligomers in solutions and in thin films. [a]measured relative to a Fc/Fc^+ redox couple as an external reference. [b]estimated from the onset of thin-film absorption.

Compd	λ_{max}abs. (sol) (nm)	λ_{max}abs. (film) (nm)	$E_{ox(onset)}$ [a] (V)	$E_{red(onset)}$ [a] (V)	E_{HOMO} (eV)	E_{LUMO} (eV)	$E_{g(cv)}$ (eV)	$E_{g(opt)}$ [b] (eV)
DTFBT	449, 632	478,680,767(sh)	0.73	-1.09	-5.53	-3.71	1.82	1.52
DTFBTz	441, 633	465,679,759(sh)	0.80	-1.00	-5.60	-3.80	1.80	1.51
DTFB2T	475, 650	504,712,791(sh)	0.68	-1.08	-5.48	-3.72	1.76	1.46
D2TFBT	466, 630	482,626,763(sh)	0.63	-1.21	-5.43	-3.59	1.84	1.48

Journal of Materials Chemistry C Accepted Manuscript

This journal is © The Royal Society of Chemistry 20xx

Please do not adjust margins

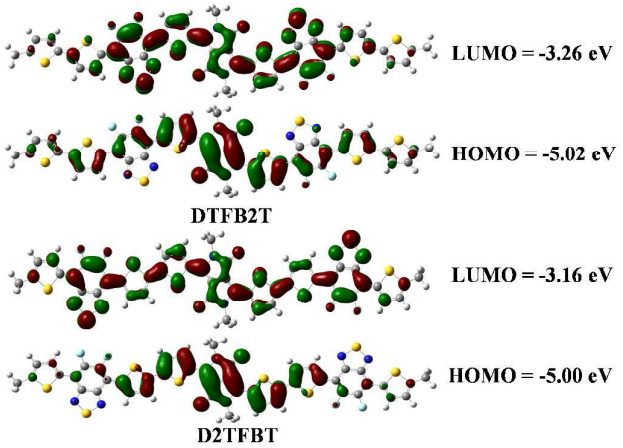

Figure 4. Comparison of HOMO and LUMO orbital surfaces, calculated energy levels of two isomers using DFT method.

From the above study, it indicated that the **D2TFBT** has two phase-transition temperatures. Therefore, we assume that the **DTBFT** possesses the liquid crystal properties. The LC properties were investigated by Optical Polarizing Microscopy (OPM) and X-Ray Diffraction (XRD) studies. The POM textures of the compound **DTFB2T** and **D2TFBT**, are shown in Figure 7. An enantiotropic optical anisotropy with a schlieren-like structure of **D2TFBT** emerges when cooled about 180 ^{o}C, suggesting the nature of the liquid-crystalline phase. And it generated a large area of the liquid-crystalline phase about 100 ^{o}C and the sample is very fluid. Finally, this texture was still observed at low temperatures, supporting a liquid crystal glass. However, we did not observe such behaviours in **DTFB2T**.

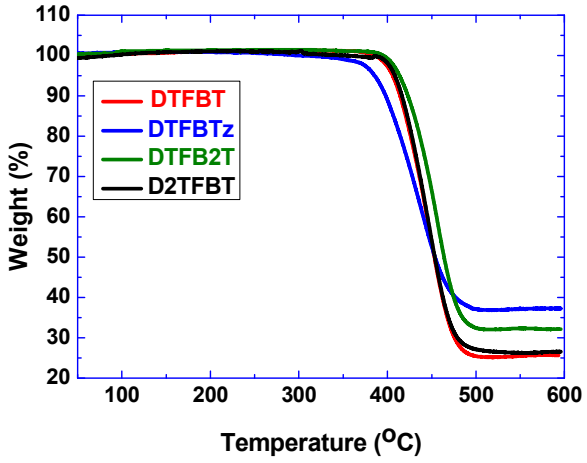

Figure 5. Thermogravimetric analysis (TGA) of **DTFBT**, **DTFBTz**, **DTFB2T** and **D2TFBT** with a heating rate of 10 ^{o}C/min under N_2 atmosphere.

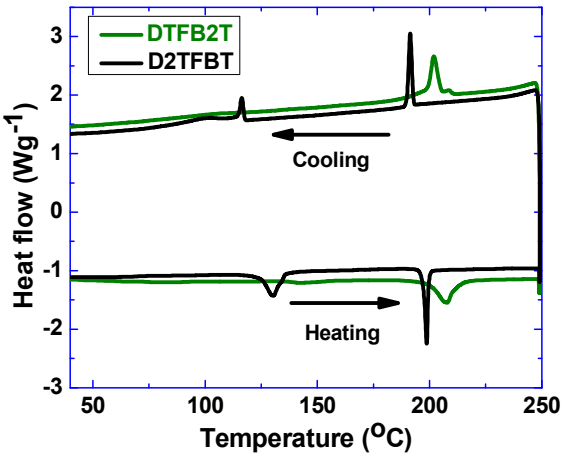

Figure 6. The second heating and cooling DSC curves of isomers **DTFB2T** and **D2TFBT** at a heating and cooling rate of 10 ^{o}C min^{-1} under N_2.

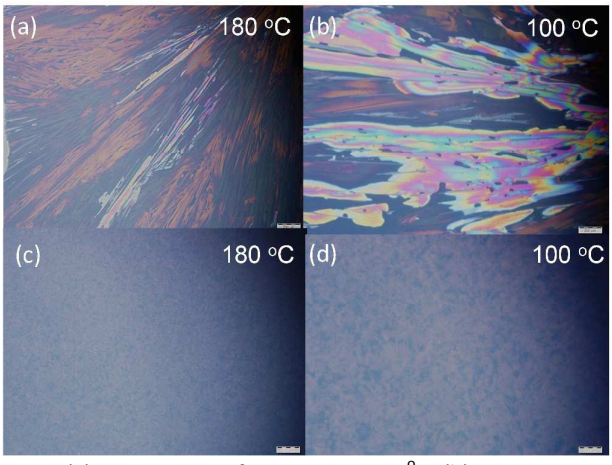

Figure 7. (a) POM image of **D2TFBT** at 180 ^{o}C. (b) POM image at 100 ^{o}C. (c) POM image of **DTFB2T** at 180 ^{o}C. (d) POM image at 100 ^{o}C.

In order to further exploration phase structures of **D2TFBT**, variable-temperature X-ray diffraction (XRD) was measured, as shown in Figure 8 and Figure S2 (4^{o}-30^{o} (2ϑ)). For (a), when the temperature reached 220 ^{o}C, there was not any reflections peaks due to the isotropic liquid. However, for (b), the temperature was cooling to 180 ^{o}C from isotropic liquid, a few distinct peaks was observed in small-angle regime. For example, a sharp reflection at 2ϑ of 5.5^{o} is appeared due to the long-range intermolecular ordered pile, which is typical pattern for a Smectic (Sm) liquid crystal phase.[53] By quenching the sample to 100 ^{o}C from the Sm phase, it formed a glass state and showed a obvious XRD pattern in figure 8 (c) that the diffractions still exists. Moreover, the molecular schlieren in the liquid crystal phase were also well maintained in the solid state. This shows that the **D2TFBT** may be a good material of liquid crystals. However, the **DTFB2T** didn't appear obvious diffractions in XRD (Figure S2). There were not any reflections peaks at 220 ^{o}C. While the temperature was cooling to 180 ^{o}C

Journal of Materials Chemistry C Accepted Manuscript

Please do not adjust margins

and 100 °C, it still not appeared any diffraction peak. That is to say that the **DTFB2T** don't have liquid crystals properties. The possible reason is that introduction the thiophene unit between the DPP and difluorobenzothiadiazole leads to a further bend into the molecular structure, which could change the molecular assembly and mesomorphic properties in the solid states.[54-57] These results can direct us to design and synthesis with the materials of liquid crystal properties by modulating the sequence of building blocks.

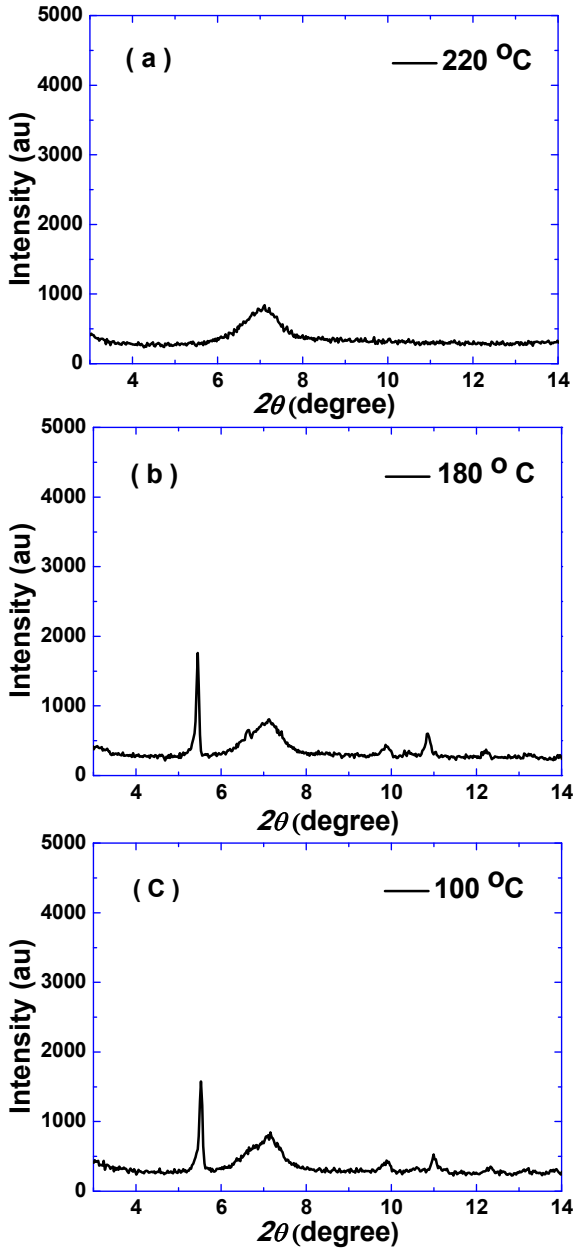

Figure 8. XRD patterns of **D2TFBT** (a) at 220 °C, (b) at 180 °C, (c) at 100 °C. The peak at about 7° denotes reflection from the peak of background.

Conclusions

In conclusion, a family of DPP-based, conjugated oligomers with difluorobenzothiadiazole as the second accepting unit have been synthesized. These oligomers showed a broad and strong absorption band (300～900 nm) and low-lying HOMO energy levels (-5.41～-5.60 eV) due to D-A interaction and multiple fluorine substituents. In combination with theoretical calculations, we have revealed that how large impacts on the photophysical and electrochemical properties, and liquid crystal properties by increasing or decreasing the ability of electron-donor groups and exchanging the moiety sequence in these materials. As compared with the isomer **D2TFBT**, **DTFB2T** with bithiophene as terminal group displays a higher melting point, dramatically red-shifted absorption spectra, and an obviously low-lying HOMO and LUMO. These results make these oligomers as promising candidate for the design of new organic electronic materials.

Experimental Section

General Procedures. All air and water sensitive reactions were performed under nitrogen atmosphere. Tetrahydrofuran (THF) was dried over Na/benzophenone ketyl and freshly distilled prior to use. Diisopropylamine was distilled from potassium hydroxide prior to use. The other materials were of the common commercial level and used as received. Thin layer chromatography (TLC) was conducted on flexible sheets precoated with SiO_2 and the separated products were visualized by UV light. Column chromatography was conducted using SiO_2 (300 mesh) from Fisher Scientific. ^1H and ^{13}C NMR spectra were recorded on a Bruker ARX-400 (400 MHz) or ARX-500 (500 MHz) spectrometer. All chemical shifts were reported in parts per million (ppm). ^1H NMR chemical shifts were referenced to TMS (0 ppm) or $CHCl_3$ (7.26 ppm), and ^{13}C NMR chemical shifts were referenced to $CDCl_3$ (77.23 ppm). MALDI-TOF-MS was recorded on a Bruker BIFLEX III mass spectrometer. Thermal gravity analyses (TGA) were carried out on a TA Instrument Q600 analyzer and differential scanning calorimetry analyses (DSC) were performed on a METTLER TOLEDO Instrument DSC822 calorimeter. Elemental analyses were performed using a German Vario EL III elemental analyzer. Absorption spectra were recorded on PerkinElmer Lambda 750 UV-vis spectrometer. Cyclic voltammetry (CV) was performed on BASI Epsilon workstation. Glassy carbon electrode was used as a working electrode and a platinum wire as a counter electrode, These films were drop-cast on a glass carbon working electrode from THF at a concentration of 5 mg/mL. Measurements were carried out at a scan rate of 50 mV/s in CH_3CN containing 0.1 M n-Bu_4NPF_6 as the supporting electrolyte. All potentials were recorded versus Ag/AgCl reference electrode and calibrated with the redox couple of Fc/Fc^+ under the same experimental conditions. The density functional theory (DFT) calculations of these molecules on their electronic states are performed using the Gaussian 09 program. The long alkyl chains were replaced by methyl groups

Journal of Materials Chemistry C Accepted Manuscript

This journal is © The Royal Society of Chemistry 20xx

Please do not adjust margins

for simplicity. The polarizing optical microscopy (POM) study was carried out on a Nikon optical polarizing microscope equipped with a Mettler Toledo FP900 hot stage. Each powder-like sample was placed on a glass slide and covered with another glass cover slip. The phase composition and purity of the as-prepared samples were analyzed by powder X-ray diffraction (XRD) with Cu Kα (λ= 1.54178 Å) incident radiation using a Shimadzu XRD-6000 at 40 kV voltage and 50 mA current. The scanning range and step of XRD pattern were 1 °-30 ° (2ϑ), 10 ° min^{-1} and 5 °C min^{-1}, respectively.

Synthesis of 2: In a 100 mL two-neck round-bottom flask, tributyl(5-hexylthiophen-2-yl)stannane (1.35 g, 3.00 mmol), 4,7-dibromo-5,6-difluorobenzo[c][1,2,5]thiadiazole (**1**) (1.0 g, 3.05 mmol) and $Pd_2(dba)_3$ (0.13 g, 0.15 mmol), tri(*o*-tolyl)phosphine (0.18 g, 0.60 mmol) was added. The flask was evacuated and back-filled with N_2 three times, and then degassed toluene (60 mL) was injected into the mixture. The resulting solution was stirred at room temperature for 12 h under the N_2 atmosphere. The solvents were then removed under reduced pressure. The dark residue was purified by silica gel chromatography, eluting with petroleum ether (PE)-CH_2Cl_2 (40:1) to give yellow solid (0.65 g, 51%). ^{1}H NMR ($CDCl_3$, 400 MHz, ppm): δ 8.07-8.06 (d, *J* = 3.6 Hz, 1H, Th-H), 6.93-6.92 (d, *J* = 3.6 Hz, 1H, Th-H), 2.92-2.88 (t, *J* = 7.6 Hz, 2H, CH_2), 1.79-1.72 (m, 2H, CH_2), 1.44-1.32 (m, 6H, CH_2), 0.92-0.88 (t, *J* = 6.8 Hz, 3H, CH_3). ^{13}C NMR ($CDCl_3$, 100 MHz, ppm): δ (153.9, 153.7, 151.4, 151.2, dd, $^1J_{CF}$ = 255 Hz, $^2J_{CF}$ = 20 Hz), (151.05, 150.98, d, $^4J_{CF}$ = 7 Hz), (150.3, 150.1, 147.7, 147.5, dd, $^1J_{CF}$ = 260 Hz, $^2J_{CF}$ = 19.1 Hz), (150.1, 150.0, d, $^4J_{CF}$ = 6 Hz), (148.1, 148.0, d, $^3J_{CF}$ = 8 Hz), (131.84, 131.75, d, $^3J_{CF}$ = 9 Hz), (128.41, 128.38, 128.35, 128.32, dd, $^3J_{CF}$ = 6 Hz, $^4J_{CF}$ = 3 Hz), 125.1, (113.9, 113.8, d, $^2J_{CF}$ = 11 Hz), (96.4, 96.2, d, $^2J_{CF}$ = 22 Hz), 31.8, 31.7, 30.3, 29.1, 22.8, 14.3. HR-ESI-MS (*m/z*): calcd for $C_{16}H_{15}BrF_2N_2S_2$: 415.9828 (100%). Found: 415.9828 (M^+, 100%).

Synthesis of 3: In a 100 mL two-neck round-bottom flask, 2-hexyl-5-(tributylstannyl)thiazole (1.38 g, 3.00 mmol), 4,7-dibromo-5,6-difluorobenzo[c][1,2,5]thiadiazole (**1**) (1.0 g, 3.05 mmol) and $Pd_2(dba)_3$ (0.13 g, 0.15 mmol), tri(o-tolyl) phosphine (0.18 g, 0.60 mmol) was added. The flask was evacuated and back-filled with N_2 three times, and then degassed toluene (70 mL) was injected into the mixture. The resulting solution was stirred at room temperature for 12 h under the N_2 atmosphere. The solvents were then removed under reduced pressure. The dark residue was purified by silica gel chromatography, eluting with PE-CH2Cl2 (1:1) to give yellow solid (0.60 g, 48%). ^{1}H NMR ($CDCl_3$, 400 MHz, ppm): δ 8.77 (s, 1H, Tz-H), 3.12-3.09 (t, *J* = 7.6 Hz, 2H, CH_2), 1.92-1.85 (m, 2H, CH_2), 1.48-1.25 (m, 6H, CH_2), 0.92-0.88 (t, *J* = 6.8 Hz, 3H, CH_3). ^{13}C NMR ($CDCl_3$, 100 MHz, ppm): δ (175.22, 175.18, d, $^4J_{CF}$ = 5 Hz), (153.5, 153.3, 151.4, 151.3, dd, $^1J_{CF}$ = 256 Hz, $^2J_{CF}$ = 20 Hz), (150.6, 150.4, 148.5, 148.3, dd, $^1J_{CF}$ = 256 Hz, $^2J_{CF}$ = 20 Hz), (150.1, 150.0, d, $^4J_{CF}$ = 5 Hz), (147.84, 147.77, d, $^3J_{CF}$ = 9 Hz), (145.9, 145.8, d, $^3J_{CF}$ = 12 Hz), 125.2, (111.6, 111.4, d, $^2J_{CF}$ = 13 Hz), (98.2, 98.0, d, $^2J_{CF}$ = 20 Hz), 33.7, 31.7, 30.1, 29.0, 22.7, 14.2. HR-ESI-MS (m/z): calcd for $C_{15}H_{14}BrF_2N_3S_2$: 416.9781(100%). Found: 417.9857 ($[M+H]^+$, 100%).

Synthesis of 5: To a solution of lithium diisopropylamide in anhydrous THF (10 mL, 1.64 mmol) was added a solution of **4** (0.40 g, 0.41 mmol) in anhydrous THF (20 mL) dropwise in N_2 atmosphere at −78 ° C. The mixture was stirred at −78 °C for 1 h and Me_3SnCl (0.24 g, 1.23 mmol) in anhydrous THF (10 mL) was added. The mixture solution was warmed up to room temperature and stirred for 10 h. The mixture solution was quenched with water, and extracted with chloroform. The organic extracts were washed with brine and dried over anhydrous Na_2SO_4. After removal of the solvents under the reduced pressure, the product was obtained as red oil (0.49 g, 91%) and used in the next step without any further purification. ^{1}H NMR ($CDCl_3$, 400 MHz, ppm): 8.98-8.97 (d, *J* = 3.6 Hz, 2H, Th-H), 7.32-7.31 (d, *J* = 3.6 Hz, 2H, Th-H), 4.05-4.03 (d, *J* = 7.6 Hz, 4H, N-CH_2), 1.91 (m, 2H, CH), 1.21 (m, 80H, CH_2), 0.89-0.87 (m, 12H, CH_3), 0.44 (s, 18H, CH_3). ^{13}C NMR ($CDCl_3$, 100 MHz, ppm): δ 162.0, 146.0, 140.1, 136.3, 136.2, 135.5, 107.5, 46.4, 38.1, 32.1, 31.6, 30.3, 29.92, 29.88, 29.83, 29.58, 29.57, 26.6, 22.9, 14.3, -7.9. HR-ESI-MS (*m/z*): calcd for $C_{68}H_{120}N_2O_2S_2Sn_2$: 1298.6829 (100%). Found: 1299.6900 (M^+, 100%).

Synthesis of 7: In a 100 mL two-neck round-bottom flask, **2** (0.30 g, 0.72 mmol), 2-tributyltinthiophene (0.19 g, 1.44 mmol), $Pd_2(dba)_3$ (33 mg, 0.036 mmol), tri(*o*-tolyl)phosphine (44 mg, 0.14 mmol) was added. The flask was evacuated and back-filled with N_2 three times, and then degassed toluene (50 mL) was injected into the mixture. The resulting solution was stirred at room temperature for 12 h under the N_2 atmosphere. The solvents were then removed under reduced pressure. The dark residue was purified by silica gel chromatography, eluting with PE-CH_2Cl_2 (30:1) to give yellow solid (0.27 g, 90%). ^{1}H NMR ($CDCl_3$, 400 MHz, ppm): δ 8.28-8.27 (d, *J* = 3.6 Hz, 1H, Th-H), 8.11-8.10 (d, *J* = 3.6 Hz, 1H, Th-H), 7.61-7.60 (d, *J* = 4.8 Hz, 1H, Th-H), 7.28-7.26 (m, 1H, Th-H), 6.95-6.94 (d, *J* = 3.6 Hz, 1H, Th-H), 2.94-2.90 (t, *J* = 7.6 Hz, 2H, CH_2), 1.81-1.73 (m, 2H, CH_2), 1.44-1.32 (m, 6H, CH_2), 0.92-0.89 (t, *J* = 6.8 Hz, 3H, CH_3). ^{13}C NMR ($CDCl_3$, 100 MHz, ppm): δ (151.5, 151.3, 148.9, 148.7, dd, $^1J_{CF}$ = 257 Hz, $^2J_{CF}$ = 19 Hz), (150.9, 150.7, 148.3, 148.1, dd, $^1J_{CF}$ = 257 Hz, $^2J_{CF}$ = 19 Hz), (150.37, 150.31, d, $^4J_{CF}$ = 6 Hz), (149.08, 149.04, 148.99, 148.94, dd, $^3J_{CF}$ = 9 Hz, $^4J_{CF}$ = 4 Hz), (131,9, 131.8, 129.1, 129.0, dd, $^1J_{CF}$ = 277 Hz, $^2J_{CF}$ = 10 Hz), (131.34, 131.25, $^3J_{CF}$ = 9 Hz), (131.91, 131.87, 131.85, 131.81, $^3J_{CF}$ = 6 Hz, $^4J_{CF}$ = 4 Hz,), (131.34, 131.25, $^3J_{CF}$ = 9 Hz), (130.83, 130.75, $^3J_{CF}$ = 8 Hz), (129.14, 129.11, 129.08, 129.05, $^3J_{CF}$ = 6 Hz, $^4J_{CF}$ = 3 Hz), 127.5, 124.9, (112.3, 112.2, d, $^2J_{CF}$ = 12 Hz), (111.2, 111.1, d, $^2J_{CF}$ = 13 Hz), 31.8, 31.7, 30.3, 29.1, 22.8, 14.3. HR-ESI-MS (m/z): calcd for $C_{20}H_{18}F_2N_2S_3$: 420.0600 (100%). Found: 421.0678 ($[M+H]^+$, 100%).

Synthesis of 8: To a solution of **7** (0.21 g, 0.50 mmol) in anhydrous THF (50 mL) was added a solution of lithium diisopropylamide in THF (10 mL, 1.0 mmol) dropwise in N_2 atmosphere at -78 °C. The mixture was stirred at −78 °C for 1 h and Me_3SnCl (0.20 g, 1.0 mmol) in anhydrous THF (10 mL) was added. The mixture solution was warmed up to room temperature and stirred for 10 h. The mixture solution was quenched with water, and extracted with chloroform. The

Journal of Materials Chemistry C Accepted Manuscript

Please do not adjust margins

organic extracts were washed with brine and dried over anhydrous Na_2SO_4. After removal of the solvent under the reduced pressure, the resulting crude product was recrystallized from methanol and chloro- form to afford the target product as red solid (0.28 g, 95%).^{1}H NMR ($CDCl_3$, 400 MHz, ppm): δ 8.33-8.32 (d, *J* = 3.6 Hz, 1H, Th-H), 8.10-8.09 (d, *J* = 3.6 Hz, 1H, Th-H), 7.35-7.34 (d, *J* = 3.6 Hz, 1H, Th-H), 6.94-6.93 (d, *J* = 3.6 Hz, 1H, Th-H), 2.94-2.90 (t, *J* = 7.6 Hz, 2H, CH_2), 1.81-1.73 (m, 2H, CH_2), 1.42-1.33 (m, 6H, CH_2), 0.92-0.89 (t, *J* = 7.0 Hz, 3H, CH_3), 0.52-0.38 (t, *J* = 28.8 Hz, 9H, $Sn(CH_3)_3$). ^{13}C NMR ($CDCl_3$, 100 MHz, ppm): δ (151.0, 150.8, 148.5, 148.3, dd, $^1J_{CF}$ = 256 Hz, $^2J_{CF}$ = 19 Hz), (150.2, 150.1, d, $^3J_{CF}$ = 6 Hz), (149.16, 149.07, 149.04, 148.94, dd, $^3J_{CF}$ = 12 Hz, $^4J_{CF}$ = 7 Hz), (142.57, 142.51, $^3J_{CF}$ = 6 Hz), (137.32, 137.29, 137.26, 137.23, dd, $^3J_{CF}$ = 6 Hz, $^4J_{CF}$ = 3 Hz), 135.53, (131.59, 131.51, $^3J_{CF}$ = 8 Hz), (131.18, 131.09, $^3J_{CF}$ = 9 Hz), (129.26, 129.22, 129.20, 129.16, dd, $^3J_{CF}$ = 6 Hz, $^4J_{CF}$ = 4 Hz), 124.9, (112.0, 111.8, d, $^2J_{CF}$ = 12 Hz), (111.4, 111.2, d, $^2J_{CF}$ = 14 Hz), 31.8, 31.7, 30.3, 29.1, 22.8, 14.3, -7.9. HR-ESI-MS (m/z): calcd for $C_{23}H_{26}F_2N_2S_3Sn$: 584.0248 (100%). Found: 584.0216 (M^+, 100%).

Synthesis of DTFBT: In a 100 mL two-neck round-bottom flask, **5** (0.13 g, 0.10 mmol), **2** (0.11 g, 0.25 mmol), and $Pd_2(dba)_3$ (4.6 mg, 0.005 mmol), tri(*o*-tolyl) phosphine (6.1 mg, 0.02 mmol) was added. The flask was evacuated and back-filled with N_2 three times, and then degassed toluene (40 mL) was injected into the mixture. The resulting solution was stirred at refluxing temperature for 12 h under the N_2 atmosphere. After being cooled to room temperature, the solvents were then removed under reduced pressure. The dark residue was purified by silica gel chromatography, eluting with PE-CH_2Cl_2(1:1) to give dark solid (0.14 g, 86%). ^{1}H NMR ($CDCl_3$, 400 MHz, ppm): δ 9.26-9.25 (d, *J* = 3.6 Hz, 2H, Th-H), 8.28-8.27 (d, *J* = 3.6 Hz, 2H, Th-H), 7.99-7.98 (d, *J* = 3.6 Hz, 2H, Th-H), 6.79-6.78 (d, *J* = 3.6 Hz, 2H, Th-H), 4.12-4.10 (d, *J* = 7.2 Hz, 4H, N-CH_2), 2.79-2.76 (t, *J* = 7.6 Hz, 4H, CH_2), 2.03 (m, 2H, CH), 1.71-1.67 (m, 4H, CH_2), 1.43-1.20 (m, 92H, CH_2), 0.93-0.81 (m, 18H, CH_3). ^{13}C NMR ($CDCl_3$, 100 MHz, ppm): δ 161.3, (151.0, 150.9, 148.5, 148.4, J_{CF} = 250, 7 Hz), (148.7, 148.6, J_{CF} = 10 Hz), 139.5, 137.0, 136.6, (132.3, 132.2, J_{CF} = 6 Hz), 131.3, 131.2, 131.1, (129.13, 129.06, J_{CF} = 7 Hz), 124.8, (112.7, 112.5, J_{CF} = 12 Hz), (109.7, 109.6, J_{CF} = 11 Hz), 109.2, 47.0, 38.8, 32.19, 32.17, 31.8, 31.6, 31.4, 30.6, 30.2, 30.1, 30.0, 29.9, 29.69, 29.65, 29.2, 26.6, 22.9, 22.8, 14.31. MALDI-TOF MS (*m/z*): calcd for $C_{94}H_{132}F_4N_6O_2S_6$: 1644.9 (100%). Found: 1533.8 ([M-C_8H_{17}+H]$^+$, 100%), 1555.8 ([M-C_8H_{17}+Na]$^+$, 100%), 1589.9 ([M-C_4H_9+H]$^+$, 100%), 1612.9 ([M-C_4H_9+Na]$^+$, 100%). Elemental Analysis: calcd for $C_{94}H_{132}F_4N_6O_2S_6$: C, 68.57; H, 8.08; N, 5.10. Found: C, 68.69; H, 7.85; N, 5.25.

Synthesis of DTFBTz: In a 100 mL two-neck round-bottom flask, **5** (0.15 g, 0.12 mmol), **3** (0.13 g, 0.29 mmol), and $Pd_2(dba)_3$ (5.5 mg, 0.006 mmol), tri(*o*-tolyl) phosphine (3.7 mg, 0.012 mmol) was added. The flask was evacuated and back-filled with N_2 three times, and then degassed toluene (40 mL) was injected into the mixture. The resulting solution was stirred at refluxing temperature for 12 h under the N_2 atmosphere. After being cooled to room temperature, the solvents were then removed under reduced pressure. The dark residue was purified by silica gel chromatography, eluting with PE-CH_2Cl_2(1:2) to give dark solid (0.15 g, 76%). ^{1}H NMR ($CDCl_3$, 400 MHz, ppm): δ 9.26-9.25 (d, *J* = 4.0 Hz, 2H, Th-H), 8.64 (s, 2H, Tz-H), 8.30-8.29 (d, *J* = 4.0 Hz, 2H, Th-H), 4.10-4.08 (d, *J* = 7.2 Hz, 4H, N-CH_2), 2.95-2.92 (t, *J* = 7.6 Hz, 4H, CH_2), 2.01 (m, 2H, CH), 1.82-1.78 (m, 4H, CH_2), 1.41-1.19 (m, 92H, CH_2), 0.93-0.80 (m, 18H, CH_3). ^{13}C NMR ($CDCl_3$, 125 MHz, ppm): δ (174.93, 174.89, J_{CF} = 5 Hz), 161.3, (151.4, 151.3, 149.4, 149.2, J_{CF} = 262, 20 Hz), (150.7, 150.5, 148.6, 148.5, J_{CF} = 262, 20 Hz), (148.41, 148.33, 148.29, 148.22, J_{CF} = 13.8, 8.8 Hz), (145.5, 145.4, J_{CF} = 11.3 Hz), 139.6, 136.6, (132.9, 132.8, J_{CF} = 7.5 Hz), (131.9, 131.8, J_{CF} = 7.5 Hz), (125.74, 125.71, 125.68, 125.65, J_{CF} = 7.5, 3.8 Hz), (111.04, 110.95, J_{CF} = 11.3 Hz), (110.3, 110.2, J_{CF} = 13.8 Hz), 109.5, 47.0, 38.8, 33.6, 32.16, 32.14, 31.7, 31.58, 30.6, 30.01, 29.98, 29.96, 29.94, 29.91, 29.62, 29.60, 29.15, 26.6, 22.89, 22.88, 22.75, 14.28, 14.25. MALDI-TOF MS (*m/z*): calcd for $C_{92}H_{130}F_4N_8O_2S_6$: 1646.9 (100%). Found: 1647.9 ([M+H]$^+$, 100%), 1670.9 ([M+Na]$^+$, 100%),. Elemental Analysis: calcd for $C_{92}H_{130}F_4N_8O_2S_6$: C, 67.03; H, 7.95; N, 6.80. Found: C, 66.96; H, 7.97; N, 6.62.

Synthesis of DTFB2T: In a 100 mL two-neck round-bottom flask, 5 (0.14 g, 0.11 mmol), 6 (0.16 g, 0.33 mmol), and $Pd_2(dba)_3$ (5.0 mg, 0.0055 mmol), tri(*o*-tolyl) phosphine (6.7 mg, 0.022 mmol) was added. The flask was evacuated and back-filled with N_2 three times, and then degassed toluene (40 mL) was injected into the mixture. The resulting solution was stirred at refluxing temperature for 12 h under the N_2 atmosphere. After being cooled to room temperature, the solvents were then removed under reduced pressure. The dark residue was purified by silica gel chromatography, eluting with PE-CH_2Cl_2 (2:1) to give dark solid (145 mg, 73%). ^{1}H NMR ($CDCl_3$, 400 MHz, ppm): δ 9.21-9.20 (d, *J* = 3.6 Hz, 2H, Th-H), 8.22-8.21 (d, *J* = 3.6 Hz, 2H, Th-H), 7.96-7.95 (d, *J* = 3.6 Hz, 2H, Th-H), 6.96-6.95 (d, *J* = 3.6 Hz, 2H, Th-H), 6.93-6.92 (d, *J* = 3.6 Hz, 2H, Th-H), 6.60-6.59 (d, *J* = 3.6 Hz, 2H, Th-H), 4.03-4.02 (d, *J* = 6.0 Hz, 4H, N-CH_2), 2.66-2.64 (m, 4H, CH_2), 2.02 (m, 2H, CH), 1.44-1.20 (m, 96H, CH_2), 0.92-0.81 (m, 18H, CH_3). ^{13}C NMR ($CDCl_3$, 125 MHz, ppm): δ 161.1, (151.7, 151.5, 149.6, 149.4, J_{CF} = 263, 20 Hz), (150.4, 150.2, 148.3, 148.1, J_{CF} = 263, 20 Hz), (148.48, 148.42, 148.40, 148.35, J_{CF} = 10, 7.5 Hz), 145.3, (142.1, 142.0, J_{CF} = 8.8 Hz), 139.2, (137.1, 137.0, J_{CF} = 7.5 Hz), 136.5, 134.4, (132.24, 132.18, J_{CF} = 7.5 Hz), (132.1, 132.0, J_{CF} = 12.5 Hz), (131.4, 131.3, J_{CF} = 11.3 Hz), (129.80, 129.75, J_{CF} = 6.3 Hz), 126.2, 124.0, 122.8, (112.2, 112.1, J_{CF} = 11.3 Hz), (109.9, 109.8, J_{CF} = 11.3 Hz), 109.0, 46.9, 41.6, 38.9, 34.3, 32.6, 32.22, 32.19, 31.5, 30.8, 30.14, 30.06, 29.99, 29.70, 29.65, 29.1, 26.5, 25.7, 23.3, 23.0, 22.9, 14.4, 14.33, 14.31, 11.00. MALDI-TOF MS (*m/z*): calcd for $C_{102}H_{136}F_4N_6O_2S_8$: 1809.8 (100%). Found: 1626.6 ([M-$C_{13}H_{27}$]$^+$, 100%), 1648.6 ([M-$C_{13}H_{27}$+Na]$^+$, 100%), 1681.7 ([M-C_9H_{19}+H]$^+$, 100%). Elemental Analysis: calcd for $C_{102}H_{136}F_4N_6O_2S_8$: C, 67.66; H, 7.57; N, 4.64. Found: C, 67.46; H, 7.48; N, 4.80.

Synthesis of D2TFBT: In a 100 mL two-neck round-bottom flask, **9** (0.11 g, 0.10 mmol), **8** (0.15 mg, 0.25 mmol), and $Pd_2(dba)_3$ (4.6 mg, 0.005 mmol), tri(*o*-tolyl) phosphine (6.1 mg, 0.02 mmol) was added. The flask was evacuated and back-filled with N_2 three times, and then degassed toluene (40 mL)

Journal of Materials Chemistry C Accepted Manuscript

This journal is © The Royal Society of Chemistry 20xx

Please do not adjust margins

was injected into the mixture. The resulting solution was stirred at refluxing temperature for 12 h under the N_2 atmosphere. After being cooled to room temperature, the solvents were then removed under reduced pressure. The dark residue was purified by silica gel chromatography, eluting with PE-CH_2Cl_2(1:1) to give dark solid (0.12 g, 66%). ^{1}H NMR ($CDCl_3$, 400 MHz, ppm): δ 9.01-9.00 (d, *J* = 4.0 Hz, 2H, Th-H), 8.06-8.05 (d, *J* = 4.0 Hz, 2H, Th-H), 7.93-7.92 (d, *J* = 3.6 Hz, 2H, Th-H), 7.19-7.18 (d, *J* = 4.0 Hz, 2H, Th-H), 7.17-7.16 (d, *J* = 4.0 Hz, 2H, Th-H), 6.74-6.73 (d, *J* = 3.2 Hz, 2H, Th-H), 4.01-3.99 (d, *J* = 6.8 Hz, 4H, N-CH_2), 2.77-2.74 (t, *J* = 7.2 Hz, 4H, CH_2), 2.00 (m, 2H, CH), 1.69-1.66 (m, 4H, CH_2), 1.38-1.21 (m, 92H, CH_2), 0.93-0.82 (m, 18H, CH_3). MALDI-TOF MS (*m/z*): calcd for $C_{102}H_{136}F_4N_6O_2S_8$: 1809.8 (100%). Found: 1809.9 (M^+, 100%), 1832.9 ([M+Na]$^+$, 100%). Elemental Analysis: calcd for $C_{102}H_{136}F_4N_6O_2S_8$: C, 67.66; H, 7.57; N, 4.64. Found: C, 67.36; H, 7.51; N, 4.54.

Acknowledgements

This work was financially supported by the grants from the National Natural Science Foundation of China (21472012, 21202007); the Thousand Youth Talents Plan of China; Beijing Natural Science Foundation (2152027). The authors thank Dr. Yazhong Dai on the theoretical calculation, Prof. Dahui Zhao and Dr. Ke Shi in optical polarizing Microscopy experiments, Prof. Zhiguo Zhang in powder X-ray diffraction (XRD) experiments.

Notes and references

1. I. A. Wright, N. J. Findlay, S. Arumugam, A. R. Inigo, A. L. Kanibolotsky, P. Zassowski, W. Domagala, P. J. Skabara, *J. Mater. Chem. C*, 2014, **2**, 2674-2683.
2 P. M. Beaujuge, J. M.J. Fréchet, *J. Am. Chem. Soc*., 2011, **133**, 20009-20029.
3 A. Mishra, P. Bauerle, *Angew. Chem. Int. Ed*., 2012, **51**, 2020-2067.
4 Y. Li, *Acc. Chem. Res*., 2012, **45**, 723-733.
5 Y. Liu, J. Zhao, Z. Li, C. Mu, W. Ma, H. Hu, K. Jiang, H. Lin, H. Ade, H. Yan, *Nature Commun*., 2014, **2**, 10101-10108.
6 H. Zhou, L. Yang, W. You, *Macromolecules*, 2012, **45**, 607-632.
7 I. Osaka, T. Kakara, N. Takemura, T. Koganezawa, K. Takimiya, *J. Am. Chem. Soc*., 2013, **135**, 8834-8837.
8 J. Cao, Q. Liao, X. Du, J. Chen, Z. Xiao, Q. Zuo, L. Ding, *Energy Environ. Sci*., 2013, **6**, 3224-3228.
9 Y. Chen, X. Wan, G. Long, *Acc. Chem. Res*., 2013, **46**, 2645-2655.
10 J. E. Coughlin, Z. B. Henson, G. C. Welch, G. C. Bazan, *Acc. Chem. Res*., 2014, **47**, 257-270.
11 J. Roncali, P. Leriche, P. Blanchard, *Adv. Mater*., 2014, **26**, 3821-3838.
12 L. Bu, X. Guo, B. Yu, Y. Qu, Z. Xie, D. Yan, Y. Geng, F. Wang, *J. Am. Chem. Soc*., 2009, **131**, 13242-13243.
13 S. Shen, P. Jiang, C. He, J. Zhang, P. Shen, Y. Zhang, Y. Yi, Z. Zhang, Z. Li, Y. Li, *Chem. Mater*., 2013, **25**, 2274-2281.
14 M. P. Nikiforov, B. Lai, W. Chen, S. Chen, R. D. Schaller, J. Strzalka, J. Maser, S. B. Darling, *Energy Environ. Sci*., 2013, **6**, 1513-1520.
15 Z. Du, W. Chen, Y. Chen, S. Qiao, X. Bao, S. Wen, M. Sun, L. Han, R. Yang, *J. Mater. Chem. A*., 2014, **2**, 15904-15911.
16 S. Holliday, R. Ashraf, C. B. Nielsen, M. Kirkus, J. Rohr, C.-H. Tan, E. Collado-Fregoso, A.-C. Knall, J. R. Durrant, J. Nelson, I. McCulloch, *J. Am. Chem. Soc*., 2015, **137**, 898-904.
17 Y. Wang, X. Zhao, X. Zhan, *J. Mater. Chem. C*, 2015, **3**, 447-452.
18 C. Zhong, H. Choi, J. Kim, H. Woo, T. Nguyen, F. Huang, Y. Cao, A. J. Heeger, *Adv. Mater*. 2015, **27**, 2036-2041.
19 Y. Lin, Z.-G. Zhang, H. Bai, J. Wang, Y. Yao, Y. Li, D. Zhu, X. Zhan, *Energy Environ. Sci*., 2015, **8**, 610-616.
20 Q. Fan, Y. Liu, M. Xiao, W. Su, H. Gao, J. Chen, H. Tan, Y. Wang, R. Yang, W. Zhu, *J. Mater. Chem. C*, 2015, **3**, 6240-6248.
21 H. Iino, T. Usui, J.-I Hanna, *Nature Commun*. DOI: 10.1038/ncomms7828.
22 Y. Fu, F. Meng, M. Rowley, B. Thompson, M. Shearer, D. Ma, R. Hamers, J. Wright, S. Jin, *J. Am. Chem. Soc*. 2015, **137**, 5810-5818.
23 S. Inoue, H. Minemawari, J. Tsutsumi, M. Chikamatsu, T. Yamada, S. Horiuchi, M. Tanaka, R. Kumai, M. Yoneya, T. Hasegawa, *Chem. Mater*. 2015, **27**, 3809-3812.
24 M. Giese, L. Blusch, M. Khan, M. MacLachlan, *Angew. Chem. Int. Ed.* 2015, **54**, 2888-2910.
25 L. Pelliser, M. Manceau, C. Lethiec, D. Coursault, S. Vezzoli, G. Leménager, L. Coolen, M. DeVittorio, F. Pisanello, L. Carbone, A. Maitre, A. Bramati, E. Lacaze, *Adv. Funct. Mater*. 2015, **25**, 1719-1726.
26 P. Ravat, T. Marszalek, W. Pisula, K. Müllen, M. Baumgarten, *J. Am. Chem. Soc*. 2014, **136**, 12860-12863.
27 B. He, Z. Ren, C. Qi, S. Yan, Z. Wang, *J. Mater. Chem. C*, 2015, **3**, 6172-6177.
28 E. Allwright, D. M. Berg, R. Djemour, M. Steichen, P. J. Dale, N. Robertson, *J. Mater. Chem. C*, 2014, **2**, 7232-7238.
29 A. Cummings, D. Duong, V. Nguyen, D. Tuan, J. Kotakoski, J. Vargas, Y. Lee, S. Roche, *Adv. Mater*. 2014, **26**, 5079-5094.
30 Z. Shuai, H. Geng, W. Xu, Y. Liao, J.-M. André, *Chem. Soc. Rev.,* 2014, **43**, 2662—2679.
31 G. Chen, H. Sasabe, T. Igrashi, Z. Hong, J. Kido, *J. Mater. Chem. A*, 2015, **3**, 14517-14534.
32 L. Ye, K. Sun, W. Jiang, S. Zhang, W. Zhao, H. Yao, Z. Wang, J. Hou, *ACS Appl. Mater. Interfaces*, 2015, **7**, 9274–9280.
33 I. Deckman, M. Moshonov, S. Obuchovsky, R. Brener, G. L. Frey, *J. Mater. Chem. A*, 2014, **2**, 16746-16754.
34 Y. Hua, J. He, C. Zhang, C. Qin, L. Han, J. Zhao, T. Chen, W.-Y. Wong, W.-K. Wong, X. Zhu, *J. Mater. Chem. A*, 2015, **3**, 3103-3112.
35 X. Y. Liu, T. Usui, J. Hanna, *Chem. Mater.* 2014, **26**, 5437-5440.
36 J. Liu, Y. Sun, P. Moonsin, M. Kuik, C. M. Proctor, J. Lin, B. B. Hsu, *Adv. Mater*., 2013, **25**, 58980-5903.
37 Y. Lin, L. Ma, Y. Li, Y. Liu, D. Zhu, X. Zhan, *Adv. Energy Mater*. 2013, **3**, 1166-1170.
38 L. Fu, W. Fu, P. Cheng, Z. Xie, C. Fan, M. Shi, J. Ling, J. Hou, X. Zhan, H. Chen, *J. Mater. Chem. A*., 2014, **2**, 6589-6597.
39 L. Ma, Z. Yi, S. Wang, Y. Liu, X. Zhan, *J. Mater. Chem. C*, 2015, **3**, 1942-1948.
40 C. Yu, Z. Liu, Y. Yang, J. Yao, Z. Cai, H. Luo, G. Zhang, D. Zhang, *J. Mater. Chem. C*, 2014, **2**, 10101-10109.
41 J. Yao, Z. Cai, Z. Liu, C. Yu, H. Luo, Y. Yang, S. Yang, G. Zhang, D. Zhang, *Macromolecules,* 2015, **48**, 2039-2047.
42 D. M. Cho, S. R. Parkin, M. D. Watson, *Org. Lett*., 2005, **7**, 1067-1068.
43 L. Yuan, Y. Zhao, K. Lu, D. Deng, W. Yan, Z. Wei, *J. Mater. Chem. C*, 2014, **2**, 5842-5849.
44 I. Yutaka, U. Masashi, A. Yoshio, Masato. U. PCT Int. Appl., 2011108646.
45 L. Huo, J. Hou, H.-Y. Chen, S. Zhang, Y. Jiang, T. L. Chen, Y. Yang, *Macromolecules*, 2009, **42**, 6564-6571.

Journal of Materials Chemistry C Accepted Manuscript

Please do not adjust margins

46 J.-L. Wang, Q.-R. Yin, J.-S. Miao, Z. Wu, Z.-F. Chang, Y. Cao, R.-B. Zhang, J.-Y. Wang, H.-B. Wu, Y. Cao, *Adv. Funct. Mater*. 2015, **25**, 3514-3523.
47 S. Yum, T. K. An, X. Wang, W. Lee, M. A. Uddin, Y. J. Kim, T. L. Xu, S. Nguyen, S. Hwang, C. E. Park, H. Y. Woo, *Chem. Mater*., 2014, **26**, 2147-2154.
48 M. Zhang, X. Guo, S. Zhang, J. Hou, *Adv. Mater*. 2014, **26**, 1118-1123.
49 Y. Deng, J. Liu, J. Wang, L. Liu, W. Li, H. Tian, X. Zhang, Z. Xie, Y. Geng, F. Wang, *Adv. Mater*., 2014, **26**, 471-476.
50 K. Cai, J. Xie, D. Zhao, *J. Am. Chem. Soc*., 2014, **136**, 28-31.
51 V. S. Gevaerts, E. M. Herzig, M. Kirkus, K. H. Hendriks, M. M. Wienk, J. Perlich, P. Müller-Buschbaum, R. A. Janssen, J. *Chem. Mater*., 2014, **26**, 916-926.
52 E. Zaborova, P. Chávez, R. Bechara, P. Lévêque, T. Heiser, S. Méry, N. Leclerc, *Chem. Commun.*, 2013, **49**, 9938-9940.
53 S. Laschat, A. Baro, N. Steinke, F. Giesselmann, C. Hägele, G. Scalia, R. Judele, E. Kapatsina, S. Sauer, A. Schreivogel, M. Tosoni, *Angew. Chem. Int. Ed*. 2007, **46**, 4832-4887.
54 Y. Wang, J. Shi, J. Chen, W. Zhu, E. Baranoff, *J. Mater. Chem. C*, 2015, **3**, 7993-8005.
55 V. Kozmík, P. Polásek, A. Seidler, M. Kohout, J. Svoboda, V. Novotná, M. Glogarová, D. Pociecha, *J. Mater. Chem.*, 2010, **20**, 7430–7435.
56 H. Lu, L. Qiu, G. Zhang, A. Ding, W. Xu, G. Zhang, X. Wang, L. Kong, Y. Tian, J. Yang, *J. Mater. Chem. C*, 2014, **2**, 1386-8005.
57 Y. A. Getmanenko, S.-W. Kang, N. Shakya, C. Pokhrel, S. D. Bunge, S. Kumar, B. D. Ellman, R. J. Twieg, *J. Mater. Chem. C*, 2014, **2**, 2600-2611.

Journal of Materials Chemistry C Accepted Manuscript

This journal is © The Royal Society of Chemistry 20xx

TOC:

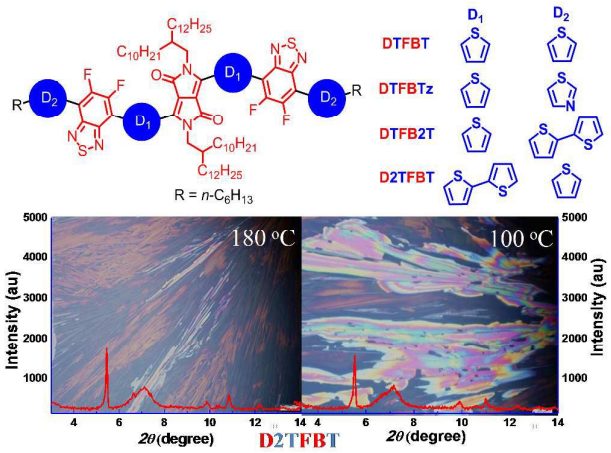

Journal of Materials Chemistry C Accepted Manuscript